Gas Processing Journal

Vol. 7, No. 1, 2019, pp. 29-40
http://gpj.ui.ac.ir

DOI: http://dx.doi.org/10.22108/gpj.2019.115824.1051

A Numerical and Thermodynamic Study on Application of a Recuperator on Thermal Efficiency and Emission of Pollutants in a Gas Power Plant

Ghodrat Ghassabi [1], Seyed Ehsan Shakib [2*], Mehran Bekri [3]

[1,2,3] Department of Mechanical Engineering, Bozorgmehr University of Qaenat, Qaen, Iran

Received: 2019-03-03 Revised: 2019-07-10 Accepted: 2019-07-16

Abstract: Over the past few years, researchers were carried out a conscious effort to explore various methods of improving the thermal efficiency of power plants. It was shown that the application of a recuperator is beneficial to improve the thermal efficiency of a gas power plant. Nevertheless, a few studies were done from a thermodynamic point of view and it is safe to say that few numerical simulation studies were performed using computational fluid dynamics. Therefore, in this study, the effect of using a recuperator was investigated to increase the temperature of the combustion chamber inlet air at four different temperatures (633, 643, 663 and 673 K) and to enhance the overall thermal efficiency. Furthermore, the effect of this approach on the emission of pollutants was explored. For this purpose, the compressor and turbine were numerically simulated using a developed MATLAB code while the combustion chamber of the gas power plant was simulated for various pre-heated temperatures in a thermodynamic analysis by ANSYS Fluent 16. The results indicated that in the case of the highest increase in the inlet air temperature to the combustion chamber (50°C) compared to the basic state (without recuperation), the thermal efficiency of the power plant and emission of nitrogen oxides were increased by 1.46% and by 44.17%, respectively.

keywords: Thermal Efficiency, Nitrogen Oxide, Combustion chamber, Computational Fluid Dynamics

1. Introduction

Increasing consumption of fossil fuels in various applications and scarcity of fossil fuel, also, the excessive discharging of pollutants has led to a situation in which the performance of fuel-consuming equipment has been closely inspected. Gas and steam power plants have a high fossil fuel consumption rate. Therefore, numerous methods have been proposed to improve their thermal efficiency and to reduce the associated fossil fuel consumption and pollutants emission. Moreover, the conversion of a gas power plant into a combined-cycle one can be regarded as one of the most common methods of improving the thermal efficiency of a power plant. However, this method requires several costly types of equipment including steam turbine, cooling tower, boiler and piping systems. Due to their simplicity and reduced costs, numerical simulation, analytical and thermodynamic approaches are rather attractive for researchers that investigate different methods of improving the performance of gas turbines.

In a research work conducted by Borat (Borat, 1982) Improvement and superiority effect of steam injection in a gas turbine), various parameters of a gas cycle were compared to those of a combined cycle (gas and steam cycle) using steam injection. This study was performed using thermodynamic analyses, and it was revealed that the cycle efficiency increases in both cases. However, this increase in efficiency was larger in the combined cycle compared to the gas cycle with steam injection. Saboonchi and Kheradmand (A.Saboonchi, & Kheradmand, 2003) have investigated the effect of changes in the geometry of the gas turbine compartment on the overall thermal efficiency using a numerical approach. The obtained results indicated that no significant changes are observed in the thermal efficiency by removing the combustion chamber elbow. In a thermodynamic analysis, Kim and Perez-

* Corresponding Author.
Authors' Email Address: Gh. Ghassabi (ghodrat.ghassabi@buqaen.ac.ir), [2] S. E. Shakib (se.shakib@buqaen.ac.ir), [3] M. Bekri (mehranbekri21@gmail.com)

ISSN (Online): 2345-4172, ISSN (Print): 2322-3251

Blanco (Kim & Perez-Blanco, 2007) have explored the effects of water injection at the compressor inlet and the application of a recuperator to increase the combustion chamber inlet temperature using the exhaust gas of the turbine. The acquired results suggested that the application of a recuperator and water injection can lead to a 6% and 270 kJ/kg increase in the thermal efficiency and net output work, correspondingly. Moreover, Sheikh Beigi and Ghofrani (Sheikhbeigi & Ghofrani, 2007) have investigated different gas turbine cycles with a reheater and a recuperator heat exchanger using a thermodynamic approach. The results revealed that using a heat exchanger improves the overall efficiency in an open cycle (heating), particularly, when the turbine inlet temperature is rather low (1000 °C). Also, in another thermodynamic analysis, De Pape et al. (De Paepe, Delattin, Bram, & De Ruyck, 2012) have simulated the effect of steam injection at the compressor outlet in a micro gas turbine cycle with a recuperator using Aspen. Furthermore, the cycle was designed in a way that the recuperator is exchanged heat with both the compressor exhaust air and the liquid water. In this research, the acquired results proposed that using a recuperator and steam injection reduce fuel consumption by 18% and increases electrical efficiency by 7%. Furthermore, in a simulated study, Zaki and Rajabi (Zaki, M., & Rajabi-Zargarabadi, 2014) have evaluated the effect of equivalence ratio on the nitrogen oxide generation in the combustion chamber for methane, propane, and pentane. The results showed that the equivalence ratio for three fuels has a significant effect on the nitrogen oxide generation. Comodi et al (Comodi, Renzi, Caresana, & Pelagalli, 2015) have examined the performance of a gas microturbine in a warm climate where the inlet air is cooled using the Vapor-Compression Refrigeration System (VCRS). The results recommended that cooling the inlet air using VCRS lead to an increase in the level of microturbine output in ISO conditions and a 1.5% upsurge in the power generation efficiency. In a thermodynamic analysis, Hassan Athari et al. (Athari, Soltani, Rosen, Kordoghli, & Morosuk, 2016) have assessed the economic exergy of a gas turbine and a combined cycle with steam injection and inlet air cooling using a nebulizer and a biomass fuel in that order. The results showed that the cooling and steam injection, as well as the steam turbine integration and gas turbine cycles, can increase the efficiency of electrical systems. Moreover, Murad Ali Pour Mohammad et al. (Pourmohamad, M. A., Ashjari, M. A., & Khosroshahi, n.d.) have scrutinized the effect of a recuperator in a microturbine system using a thermodynamic approach. The results proposed that using a recuperator can lead to a reduction in fuel consumption by 45%. EL-Shazly et al. (El-shazly, Elhelw, Sorour, & El-maghlany, 2016) have examined the improvement of an integrated gas turbine performance using various inlet cooling techniques. In this study, a gas turbine without cooling was been compared to a gas turbine with cooling (absorption refrigerator) and a water cooler in terms of thermal efficiency, power output, and fuel consumption. A significant improvement was observed in the thermal efficiency and power output of the gas turbine with cooling. It should be noted that in our study, the turbine performance was simulated using C++ and the obtained results were compared to an "MS 6001 B" turbine.

Sahu and Sanjay (Sahu, 2017) have examined the application of an intercooler in a cycle with a recuperator using a thermodynamic approach. In this cycle, layered cooling was used for the blades of the turbine. The results exposed that the specific work of the cycle with a recuperator and intercooler and the fuel consumption of this cycle are 50% and 27.8% higher compared to the base cycle, respectively.

Amiri-Rad and Kazemian-Najafabadi (Amiri-Rad & Kazemiani-najafabadi, 2017) have thermodynamically investigated a gas turbine cycle with steam injection and a recuperator to determine the optimum steam temperature. Their results showed that the optimum temperature is 318.5°C and the thermal efficiency increases by 4.6% at this temperature.

Sanaye et al. (Sanaye, Amani, & Amani, 2018) have explored a multi-objective optimization of a power plant including a gas turbine cycle with steam injection, a steam generator system, and a cooling absorbent using the genetic algorithm. The acquired findings proposed that thermal efficiency is 30.7% in optimal working conditions.

In a thermodynamic analysis, Pashchenko (Pashchenko, 2018) has evaluated the effect of using a recuperator via the heat of the turbine outlet gas. This recuperator was used for the pre-heating of steam and methane. Additionally, the steam and methane were injected into the combustion chamber after the preheating process by the recuperator. The results indicated that an increased level of pressure reduces the recuperator efficiency.

As previously mentioned, a recuperator can be employed to increase the inlet air

temperature of the combustion chamber. This approach may be considered as one of the most important proposed methods to improve the overall efficiency of a power plant. An upsurge in the inlet air temperature of the combustion chamber is associated with an increase in the overall thermal efficiency. This is because less energy is used to warm the inlet turbine gas. A large number of thermodynamic and mathematical modeling studies have been carried out in the field of heat recovery; however, there are a few conducted numerical simulation studies for comparison which were carried out by computational fluid dynamics. Furthermore, due to the complexities of a combustion process and nonlinearity of various mass fraction equations of species, the effect of this particular method on the amount of pollutant generated in the process has not been meticulously explored thus far. The main purpose of this study is to investigate the effect of recuperation on the thermal efficiency and emission of pollutants using a numerical simulation of the combustion chamber and thermodynamic analysis of other primary components of a power plant. Finally, the temperature distribution and mass fraction of species in the combustion chamber are assessed for a simple gas cycle to provide a comprehensive numerical simulation.

2. Introducing the Cycle with a Recuperator

In a simple gas power plant cycle, the mean temperature of the turbine heat output is about 550 °C [16]. This heat is released to the surrounding environment and is essentially wasted. However, this heat can be utilized to increase the inlet temperature to the combustion chamber using a recuperator. The schematic diagram of a gas power plant cycle with a recuperator is shown in Figure 1 (Cycle 1). As can be seen, the outlet compressor flow (line 2) is heated using hot exhaust gases of the power plant (line 5) in a recuperator; therefore, the air (line 3) enters the combustion chamber at a higher temperature. The increased inlet temperature of the combustion chamber causes complete combustion, increased reaction rate, and consequently increased turbine inlet temperature and work output. In this research, the effect of the recuperation on the thermal efficiency was investigated to increase the inlet air temperature of the combustion chamber. This was performed in a way that the air temperature without recuperation (basic condition) was determined at 623 K. The obtained results were then compared to a recuperator and four different elevated temperatures including 10° (633 K), 20° (643 K), 40° (663 K) and 50° (673 K) upsurge in temperature.

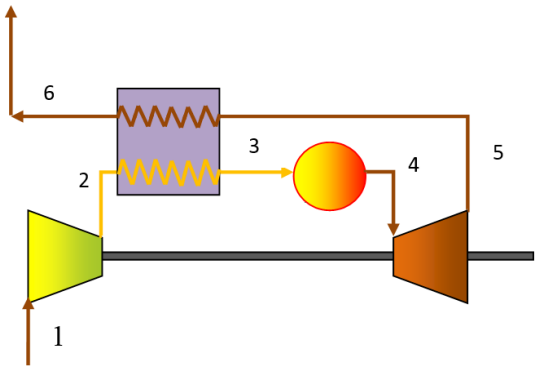

Figure 1. Schematic diagram of a gas power plant cycle with a recuperator

In this research, the combustion chamber was evaluated using numerical simulation and the compressor, turbine, and recuperator of the power plant was assessed using a developed MATLAB code in a thermodynamic analysis. The required information is presented in Table 1 where the input variables are shown in two identical cycles.

Table 1. Input variables for a simple cycle and cycle 1

Input Variable	Value
Compressor Inlet Temperature ($T1$)	295 K
Compressor outlet temperature ($T2$)	623 K
Turbine Inlet Pressure ($P4$)	830 KPa
Turbine Outlet Pressure ($P5$)	100 KPa
Mass Flow Rate of Fuel ($\dot{m}_f$)	3.64 kg/s
Mass Flow Rate of air ($\dot{m}_a$)	214.2 kg/s
Heating value of Fuel (h_f)	50010 kJ/kg

3. Governing Equations and Numerical Simulation of the Combustion Chamber

The geometry of a gas combustion chamber is shown in Figure 2. This chamber was designed with a concentric double elbow and has eight burners located in the upper part as shown in Figure 2. Additionally, the burner geometry is depicted in Figure 3. As shown in Figure 2, the air enters from the outer elbow, moves toward the upper section of the compartment, and then mix with the incoming methane from the burner. The combustion occurs when the fuel and air are mixed so that its products are transferred from the center after passing the inner elbow pathway. The dimensions of this compartment are shown in Figure 4.

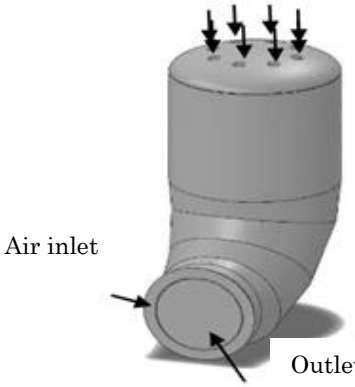

Figure 2. Combustion chamber Schematic

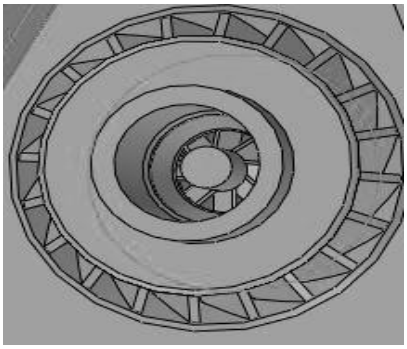

Figure 3. Schematic of a burner

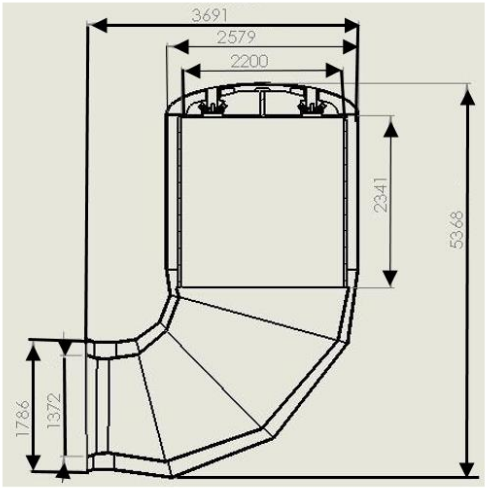

Figure 4. Combustion Chamber Dimensions (mm)

The non-premixed combustion of methane is considered. Moreover, Simple algorithm is used to solve the momentum equations and pressure discretization. The combustion flow is turbulent, and the standard k-e model is employed to model this turbulent flow. Upwind differencing scheme is applied for the discretization of all convective terms. In this model, the two transfer equations - for calculating the kinetic energy (k) and the rate of dissipation of turbulence energy (ε) - are solved as follows(Pope, 2007).

$$\frac{\partial}{\partial t}(\rho k)+\frac{\partial}{\partial x_i}(\rho k u_i) = \frac{\partial}{\partial x_i}\left(\alpha_k \mu_{eff}\frac{\partial k}{\partial x_j}\right)+G_k + G_b-\rho\varepsilon-Y_m \quad (1)$$

$$\frac{\partial}{\partial t}(\rho \varepsilon)+\frac{\partial}{\partial x_i}(\rho \varepsilon u_i) = \frac{\partial}{\partial x_i}\left(\alpha_\varepsilon \mu_{eff}\frac{\partial \varepsilon}{\partial x_j}\right)+C_{1\varepsilon}\frac{\varepsilon}{K}(G_k+C_{3\varepsilon}G_b)-C_{2\varepsilon}\rho\frac{\varepsilon^2}{K} \quad (2)$$

Where G_k denotes the generated turbulent energy due to change in mean velocity, G_b represents the generated turbulent energy owing to the buoyancy force exhibitions, Y_m is the ratio of expansion perturbation incompressible turbulence to the overall rate of turbulence energy dissipation. Based on previous studies (Pope, 2007), the constant coefficients of these equations were determined at $\alpha_\varepsilon = 0.72\,; C_\mu = 0.0845;\ \alpha_k = 072;\ C_{1\varepsilon} = 1.42;\ C_{2\varepsilon} = 1.68$

Magnussen model was used (the following equation) to determine the combustion reaction rate which is represented as a source term in the energy equation and mass fraction conservation of species(Magnussen, F. F., & Hjertager, 1976):

$$R.R = A\rho\frac{\varepsilon}{K}MIN\left(Y_f.\frac{Y_{o_2}}{S}\right) \quad (3)$$

Where R.R represents the reaction rate, A is an empirical constant (equal to 4), Y is the mass fraction of the fuel and oxygen, S is the amount of oxygen required for the combustion of one kilogram of the fuel in a stoichiometric state.

In addition, only a form of heat, which has been developed by the Zeldovich mechanism (Warnatz, J., Mass, U., & Dibble, 2006), was considered for the modeling of the nitrogen oxides (NO), and its associated reactions are as follows:

$$O+N_2 \overset{k_{\pm1}}{\leftrightarrow} NO+N$$
$$4\quad N+O_2 \overset{k_{\pm2}}{\leftrightarrow} NO+O\quad 4 \quad (4)$$
$$N+OH \overset{k_{\pm3}}{\leftrightarrow} NO+H$$

Where $K_{\pm1.2.3}$ $(\frac{m^3}{mol.s})$ are the reciprocal reaction constants expressed as follows (Hanson, R. K., & Salimian, 1984):

$$K_1 = 1.8 * 10^8 \exp(-\frac{38370}{T})$$
$$K_{-1} = 38 * 10^7 \exp(-\frac{425}{T}) \quad (5)$$
$$K_2 = 1.8 * 10^4 * \mathrm{T} * \exp(-\frac{4680}{T})$$
$$K_{-2} = 3.81 * 10^3 * \mathrm{T} * \exp(-\frac{20820}{T})$$
$$K_3 = 7.1 * 10^7 \exp(-\frac{450}{T})$$
$$K_{-3} = 1.7 * 10^8 \exp(-\frac{24560}{T})$$

Therefore, the formation rate of NO is obtained using the following equation(ANSYS, 2013):

$$\frac{d[NO]}{dt} = K_1[O][N_2] + K_2[N][O_2] + K_3[N][OH] - K_{-1}[NO][N] - K_{-2}[NO][O] - K_{-3}[NO][H] \quad (6)$$

The DO model was also considered for radiation modeling(ANSYS, 2013). The inlet boundary condition of the air and fuel are velocity inlet, furthermore, the outlet boundary condition of the combustion products is pressure outlet. Moreover, the external wall is considered to be insulated due to the insulation of the outer body of the combustion chamber.

After a series of trial and error and verifying the results for temperature near the burner as the high gradient location, to validate the independence of our results from the computational mesh, 47000 hexagonal elements were considered as the minimum number of elements for the independence of our results. Also, residual levels are considered less than 10^{-5} as the convergence criterion. The geometry of the combustion chamber and its associated computational meshwork using a Triangular type element is depicted in Figure 5.

Furthermore, for the accuracy validation of the numerical results, the mean temperature of the combustion chamber outlet obtained from the numerical simulation was compared to the data collected from Kaveh Qaen's power plant (*Performance test of Kave combined cycle PP (GT V94.2)*, n.d.) where the working condition was similar to a simple cycle used in this research as depicted in Table 2. Thus, the results revealed that the numerical solution error is less than 1% which is a strong indication of the numerical solution accuracy.

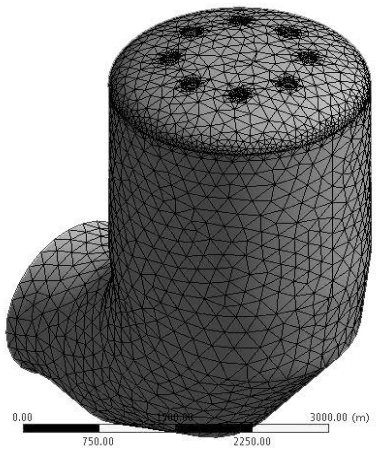

Figure 5. Computational mesh of the combustion chamber

Table 2. Comparison of numerical and empirical results

Result	Mean Outlet Temperature (K)
Numerical solution	1056
Empirical result (*Performance test of Kave combined cycle PP (GT V94.2)*, n.d.)	1060

4. Thermodynamic Analysis

In this study, the gas turbine cycle is a simple cycle which includes a compressor, a combustion chamber, and a gas turbine. Also, the behavior of the compressor, gas turbine, and waste recuperator was predicted using a code developed in MATLAB. This thermodynamic analysis was performed to determine the air temperature at the compressor, r, and gas turbine outlets.

In contrast to the air standard Joule cycle, irreversibility of practical turbo machines should be considered in the analysis of the gas turbine power plants using a simple cycle. Generally, the irreversibility of the turbo machines was determined by taking into account the associated isentropic efficiency.

The following assumptions are normally considered in simulating the actual cycle of a gas turbine:

- The cycle works in a steady state.
- In the ideal state, the inlet air has the following volume fraction composition (CLAUS BORGNAKKE, 2009):

$$0.7748N_2 + 0.2059O_2 + 0.0003CO_2 + 0.019H_2O \quad (7)$$

- The ideal gas law was used for the air and combustion products.
- Compressor and turbine were considered adiabatic.
- Methane was the primary source of energy.
- The atmospheric air temperature in the compressor was increased isentropically based on the following equation(CLAUS BORGNAKKE, 2009):

$$\int C_p \frac{dT}{T} = \frac{R}{\eta_p} \ln\left(\frac{P_2}{P_1}\right) \quad (8)$$

Where T is the temperature in Kelvin, P is the pressure in kPa, C_p is the specific heat capacity in $kJ/kg.K$ and subscripts 1 and 2 denote the inlet and outlet conditions, respectively. Moreover, η_p is the polytropic efficiency of the compressor. The specific heat capacity, enthalpy, and entropy values of every single element were calculated using the following equation as a function of

temperature(Bejan, A., Tstsaroincs, G., & Moran, 1996).

$$C_p = a + by + cy^{-2} + dy^2 \quad (9)$$

$$h = 10^3 \left[H^+ + ay + \frac{b}{2}y^2 - cy^{-1} + \frac{d}{3}y^3\right] \quad (10)$$

$$s = S^+ + a\ln(T) + by - \frac{c}{2}y^{-2} + \frac{d}{2}y^2 \quad (11)$$

$$y = {}^{T}/_{1000} \quad (12)$$

It should be noted that the physical properties of air should be determined in terms of the volume fraction of its constituent elements. Therefore, on condition that the humidity changes, the composition of the elements also will be varied and consequently, the physical properties altered. Hence, the physical properties of the air in the simulator code were considered as a function of the humidity and air temperature to improve the accuracy of the calculations where a, b, c, and d are constants used for each of the air element and y is a function of temperature. The values of these coefficients are given in Table 3 for nitrogen, oxygen, carbon dioxide and water (Bejan, A., Tstsaroincs, G., & Moran, 1996).

Table 3. values of a, b, c, and d for different air elements

Element	a	b	c	d
Nitrogen	30.418	2.544	0.238	0
oxygen	29.154	6.477	0.184	1.017
Carbon dioxide	51.128	4.368	1.469	0
Water	34.376	7.841	0.423	0

Similar to the previously mentioned equations for the compressor, the gas turbine outlet temperature was calculated using the following equation (CLAUS BORGNAKKE, 2009):

$$\int C_p \frac{dT}{T} = R\eta_p \ln\left(\frac{P_4}{P_5}\right) \quad (13)$$

where the subscripts 4 and 5 refer to the turbine inlet and outlet, respectively. Energy balance written for the waste recuperator is presented as follows (CLAUS BORGNAKKE, 2009):

$$\dot{m}_a(h_3 - h_2) = \dot{m}_g(h_5 - h_6) \quad (14)$$

$$p_3 = p_3(1 - \Delta p_{APH}) \quad (15)$$

where the subscripts 5 and 6 correspond to the inlet and outlet of the recuperator, respectively. Moreover, Δp_{APH} is related to the air pressure drop in the recuperator.

It should also be noted that the primary goal of modeling a gas turbine cycle is the ability to predict the behavior of the cycle to determine the flow rate and exhaust gas temperature from the turbine under different conditions.

5.1. Results

5.1. Numerical Simulation Results of the Combustion Chamber for a Simple Cycle (without Recuperator)

In this section, the numerical simulation results including the temperature distribution and mass fraction of pollutants in the combustion chamber are evaluated for a simple gas power plant. The mass fraction distribution of methane is depicted in Figure 6 in the middle section of the combustion chamber. The mass fraction is considered to be unity due to the presence of pure methane at the flare fuel inlet. At the flared outlet, the value of the fuel mass fraction was sharply dropped due to mixing with the air and combustion process and most of the fuel was consumed. As a result, the fuel mass fraction is quite negligible in large parts of the combustion chamber.

Figure 7 shows the distribution of the oxygen mass fraction in the middle section of the combustion chamber. Oxygen was not consumed until the flare and the mass fraction was considered to be unity. The oxygen mass fraction is about 0.23 in the air while nitrogen almost takes up the rest. Moreover, due to the air passage from the flare and mixing with the fuel, the combustion occurs and the available oxygen level or it's mass fraction decreases. At the gap section and after the combustion products are passed by, the oxygen mass fraction increases due to the addition of some non-combusted air. Furthermore, the mean oxygen mass fraction is around 0.158 at the outlet based on Figure 7. This excess air helps to control and reduce the turbine inlet temperature.

The temperature distribution is depicted in Figure 8 in the middle section of the combustion chamber. As can be seen, the air is mixed with the fuel and the combustion occurs in the vicinity of the flare. The temperature upsurges to 2030 K in the middle section and center of the flame. However, the interaction between the flame radiation and combustion chamber wall results in a reduction up to 600 K in the mean flame temperature. The gap inlet air is then mixed with the combustion products. Finally, the mean outlet temperature of the combustion chamber is further reduced to 1340 K.

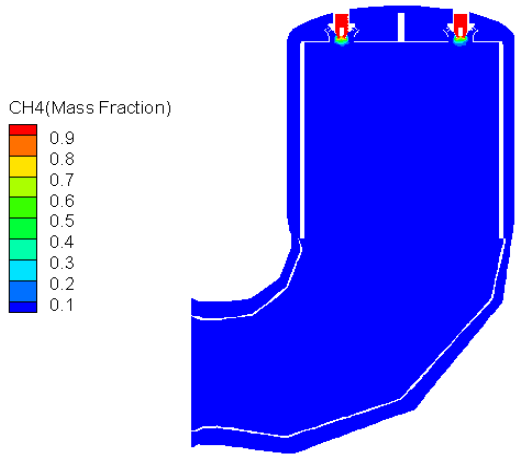

Figure 6. Distribution of methane mass fraction in the middle section of the combustion chamber

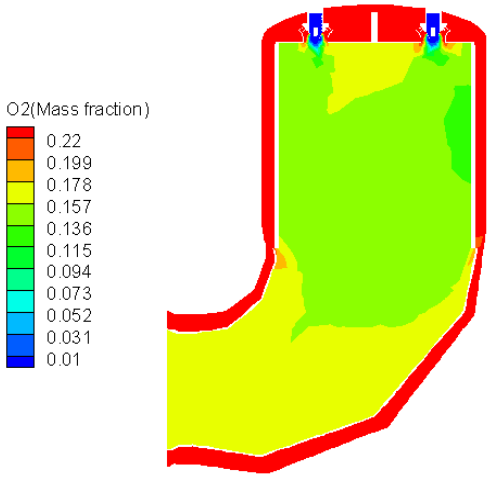

Figure 7. Distribution of the oxygen mass fraction in the middle section of the combustion chamber

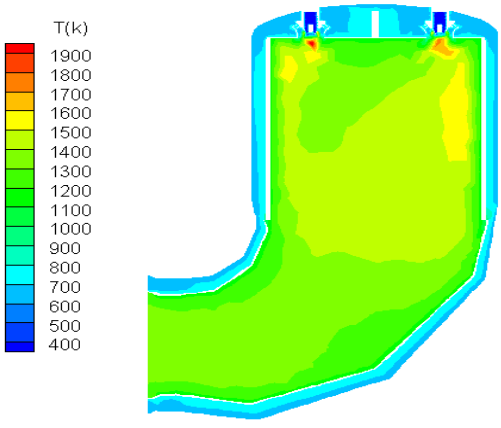

Figure 8. Distribution of temperature in the middle section of the combustion chamber

Carbon monoxide is a gas which is only produced by incomplete combustion of the carbon. Figure 9 shows the distribution of the carbon monoxide mass fraction in the middle section of the combustion chamber. It can be observed that the carbon monoxide is initially generated in the vicinity of the flare because of a sudden surge in the temperature, breakdown of the fuel molecules, and a mixture of carbon atoms and oxygen. It is worthy to note that due to an increased rate of the fuel and air mixing and the addition of excess air from the gap, carbon monoxide is gradually converted into the carbon dioxide. Consequently, the carbon monoxide mass fraction significantly decreases and is rather small at the outlet.

The distribution of the carbon dioxide mass fraction is illustrated in the middle section of the combustion chamber in Figure 10. As can be seen, the mass fraction of carbon dioxide is essentially zero owing to the lack of combustion until the flare. Moreover, due to a proper mixing of the fuel and air and complete combustion at the flared outlet and in the center of the flame, the mass fraction of the carbon dioxide is at the maximum value. Furthermore, the mass fraction of the carbon dioxide is decreased as a result of the entry of non-combusted air from the gap and its mixture with the combustion products. Consequently, these products are gradually diluted.

The distribution of the mass fraction of nitrogen oxides is presented in Figure 11 in the middle section of the combustion chamber. Because of the high temperature, nitrogen oxides are generated in the vicinity of the flare. Additionally, the dilution of the combustion products, the addition of the excess air from the gap, and the mass fraction of nitrogen oxides are decreased caused by lessening temperature. The mean value of nitrogen oxides was 0.119 ppm at the outlet.

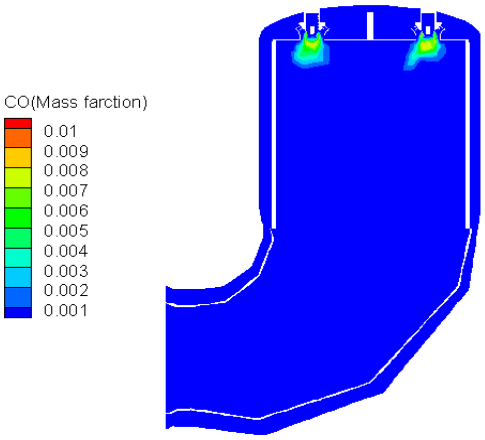

Figure 9. Distribution of carbon monoxide mass fraction in the middle section of the combustion chamber

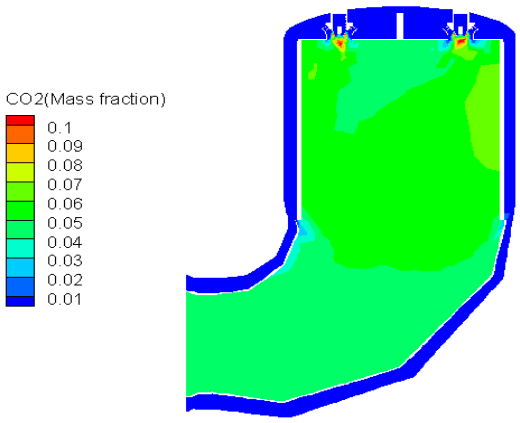

Figure 10. Distribution of carbon dioxide mass fraction in the middle section of the combustion chamber

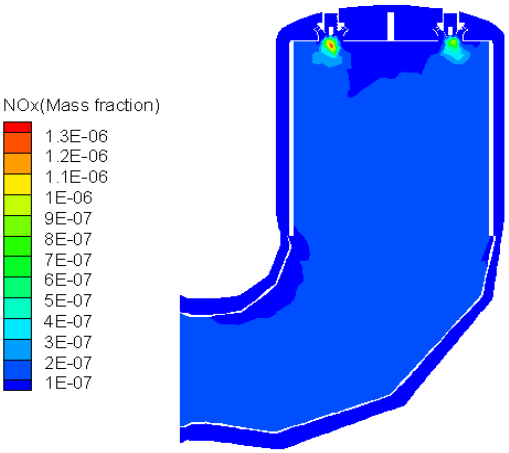

Figure 11. Distribution of nitrogen oxides mass fractions in the middle section of the combustion chamber

5.2. Effect of a Recuperator on the Temperature Distribution, Efficiency, and Emission of Pollutants

In this section, the effect of a recuperator on the temperature distribution, efficiency, and emission of pollutants is investigated. For this purpose, the effect of this unit was analyzed in terms of different preheated temperatures.

In Figure 12, the temperature contour shows a 10-degree rise in temperature. As can be seen, the air is mixed with the fuel and combustion occurs at the flare section. Since the air enters the combustion chamber with higher temperature compared to the basic state (without an increase in its initial temperature), the temperature reaches around 2050 K in the flare center. Furthermore, in the case of a 10-degree increase in the air temperature, the flame length was not significantly changed compared to the state with no temperature increase (see Figure 7). However, based on Figure 12, the temperature and mean temperature at the center of the flame and combustion chamber outlet were increased by 20°C and 10°C, respectively.

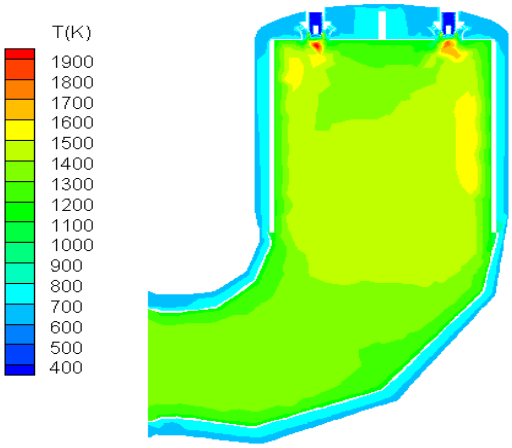

Figure 12. Temperature distribution for the case of a 10-degree increase in the air temperature in the middle section of the combustion chamber

The temperature contour, which is shown in Figure13, depicts a 20-degree increase in the air temperature that enters the combustion chamber. In this case, the flame length was relatively higher compared to that of the basic state. Moreover, the temperature and mean one at the center of the flame and combustion chamber outlet were increased by 10°C and 45°C compared to that of the basic state in that order.

As shown in Figure 14, the temperature contour presents a 40-degree upsurge in the air temperature that goes into the combustion chamber. In this case, the flame length was again relatively higher compared to that of the basic state and those temperatures, which were mentioned earlier, were increased by 20°C and 50°C, respectively.

Figure 15 shows the temperature contour of a 40-degree increase in the air temperature that enters the combustion chamber. It can be easily observed that due to this largest temperature increase (50 °C), the flame has the highest length compared to the basic state. In addition, the mean temperature at the combustion chamber outlet is 90 °C higher than the basic state.

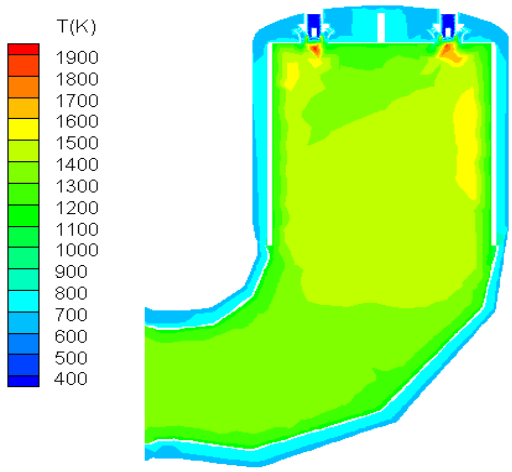

Figure 13. Temperature distribution for the case of a 20-degree increase in the air temperature in the middle section of the combustion chamber

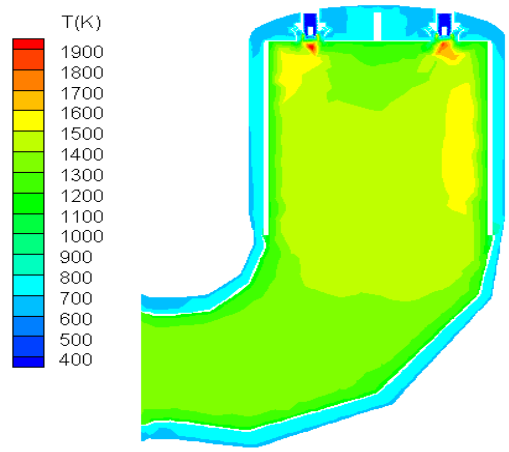

Figure 14. Temperature distribution for the case of a 40-degree increase in the air temperature in the middle section of the combustion chamber

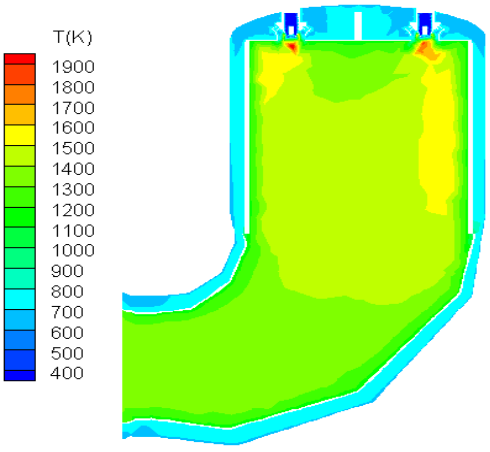

Figure 15. Temperature distribution for the case of a 50-degree increase in the air temperature in the middle section of the combustion chamber

The thermal efficiency diagram in terms of the preheating temperature is shown in Figure 16. As can be seen, when the inlet air temperature of the combustion chamber is increased, the thermal efficiency also rises linearly. The power plant efficiency was determined at 31.6% with a 10-degree rise in temperature for the basic state (623 K). This efficiency was increased to 31.97% (0.37% improvement) while it was 32.29% (0.69% improvement) for a 20-degree increase in temperature. Moreover, the efficiency was determined at 32.8% (1.2% improvement) for a 40-degree increase in temperature. According to the highest increase in temperature (i.e. 50°C), the thermal efficiency of 33.06% was achieved (1.46% improvement). As the inlet air temperature of the combustion chamber increases, the thermal efficiency is expected to enhance. This is mainly because when the inlet combustion chamber temperature increases, the turbine working temperature is also increased, which manifests in a higher turbine output, so, a higher thermal efficiency because of the increased specific volume of the turbine.

Figure 17 represents the mass fraction of nitrogen oxides (NOx) in terms of the preheating temperature. Based on the temperature in this figure, one may observe that as the air temperature increases, the number of generated nitrogen oxides is also elevated. This may be since that as the inlet air temperature into the combustion chamber upsurges, the maximum temperature of the flame also increases. Furthermore, the triple bond of the nitrogen is broken down at this temperature and the nitrogen radicals are then converted to NOx established upon various mechanisms. Therefore, when the pre-heating temperature is increased, more triple nitrogen bonds are broken down which leads to a higher number of generated NOx. In the case of maximum pre-heating, NOx is generated by 44.17% more than the basic state.

Figure 18 shows the mass fraction of the carbon dioxide in terms of temperature. Furthermore, it is significantly increased with a 10-degree increase in its temperature compared to the basic state (without recuperator). Subsequently, as the pre-heating temperature increases, the growth in the mass fraction of the carbon dioxide is rather negligible which indicates that a large increase in the preheating temperature does not have a significant effect on the complete or incomplete characteristic of the combustion. Therefore, it does not increase the mass fraction of carbon dioxide.

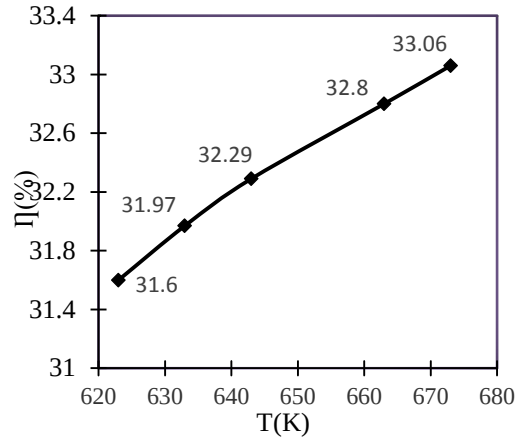

Figure 16. Thermal efficiency in terms of the preheating temperature

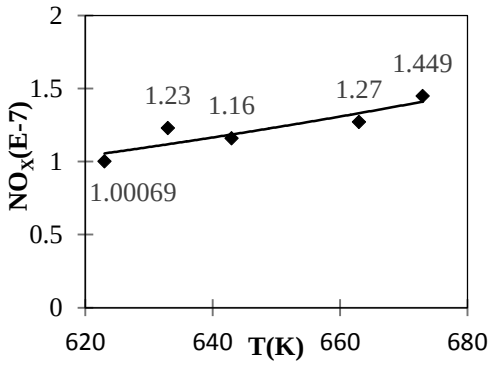

Figure 17. The nitrogen oxides mass fraction in terms of the preheating temperature

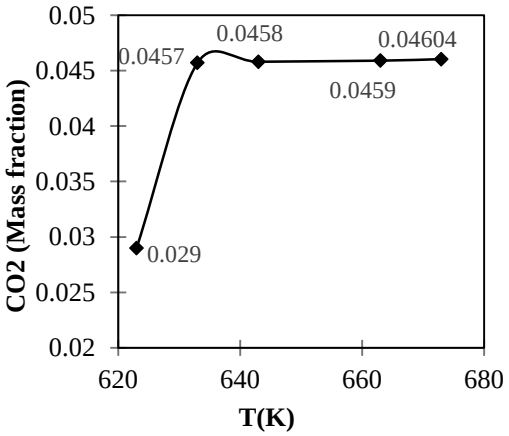

Figure 18. The carbon dioxide mass fraction diagram in terms of the preheating temperature

6. Conclusion

In this research, the effect of using a recuperator was investigated on the thermal efficiency and emission of the pollutants in a gas power plant cycle. For this purpose, the combustion chamber of a gas power plant (V94.2 gas turbine) was numerically evaluated by ANSYS Fluent 16. Moreover, the net power and thermal efficiency of the power plant were determined using a developed MATLAB code for various pre-heated temperatures in a thermodynamic analysis. In addition, in order to achieve a comprehensive numerical simulation, temperature distribution and mass fraction of combustion products in the combustion chamber were analyzed for a simple cycle of a gas power plant. The obtained results revealed the following statements despite the presence of a recuperator and in the case of maximum pre-heating:

- Thermal efficiency was increased by 1.46%.
- Net power was increased by 2.65 MW.
- Emission of NOx was increased by 44.17%.
- Carbon dioxide Emission was increased by 69.1%.

7. Symbols

A	Empirical Constant
C_p	Specific heat capacity at constant pressure $(J/kg.k)$
C_v	Specific heat capacity at constant volume $(J/kg.k)$
G_k	Generated turbulent energy due to mean velocity changes (J)
G_b	Generated turbulent energy due to buoyancy forces (J)
H	Enthalpy (J)
H_f	Heating value of Fuel (kJ/kg)
$\dot{m}_f$	Rate of fuel consumption (kg/s)
$\dot{m}_a$	Rate of air consumption (kg/s)
P	Pressure (kPa)
R.R	Reaction Rate (kg/s)
S	The amount of oxygen required for the combustion of one kilogram of the fuel in a stoichiometric state (kg)

8. References

A.Saboonchi, & Kheradmand, S. (2003). 3D-Numerical Gas Turbine Combustor. *Esteghlal*, *22*(2).

Amiri-Rad, E., & Kazemiani-najafabadi, P. (2017). Thermo-environmental and economic analyses of an integrated heat recovery steam-injected gas turbine. *Energy*. https://doi.org/10.1016/j.energy.2017.11.044

ANSYS, I. (2013). Ansys Fluent 16 User's Guide. In *Software Review*. https://doi.org/10.1016/0140-3664(87)90311-2

Athari, H., Soltani, S., Rosen, M. A., Kordoghli, M., & Morosuk, T. (2016). Exergoeconomic study of gas turbine steam injection and combined power cycles using fog inlet cooling and biomass fuel. *Renewable Energy*, *96*, 715–726. https://doi.org/10.1016/

j.renene.2016.05.010

Bejan, A., Tstsaroincs, G., & Moran, M. (1996). *Thermal design and optimization*. New York: Wiley.

Borat, O. G. U. Z. (1982). *Efficiency improvement and superiority of steam injection in gas turbines*. *22*, 13–18.

CLAUS BORGNAKKE, R. E. S. (2009). *FUNDAMENTALS OF THERMODYNAMICS* (SEVENTH ED). University of Michigan: John Wiley & Sons, Inc.

Comodi, G., Renzi, M., Caresana, F., & Pelagalli, L. (2015). Enhancing micro gas turbine performance in hot climates through inlet air cooling vapour compression technique. *APPLIED ENERGY*, *147*, 40–48. https://doi.org/10.1016/j.apenergy.2015.02.076

De Paepe, W., Delattin, F., Bram, S., & De Ruyck, J. (2012). Steam injection experiments in a microturbine - A thermodynamic performance analysis. *Applied Energy*, *97*, 569–576. https://doi.org/10.1016/j.apenergy.2012.01.051

El-shazly, A. A., Elhelw, M., Sorour, M. M., & El-maghlany, W. M. (2016). Gas turbine performance enhancement via utilizing different integrated turbine inlet cooling techniques. *Alexandria Engineering Journal*. https://doi.org/10.1016/j.aej.2016.07.036

Hanson, R. K., & Salimian, S. (1984). Survey of Rate Constants in H/N/O Systems. *Combustion Chemistry*, 361.

Kim, K. H., & Perez-Blanco, H. (2007). Potential of regenerative gas-turbine systems with high fogging compression. *Applied Energy*, *84*(1), 16–28. https://doi.org/10.1016/j.apenergy.2006.04.008

Magnussen, F. F., & Hjertager, B. H. (1976). On mathematical models of turbulent combustion with special emphasis on soot formation and combustion. *Paper Presented at the In 16th Symp. on Combustion*. The Combustion Institute.

Pashchenko, D. (2018). Energy optimization analysis of a thermochemical exhaust gas recuperation system of a gas turbine unit. *Energy Conversion and Management*, *171*(June), 917–924. https://doi.org/10.1016/j.enconman.2018.06.057

Performance test of Kave combined cycle PP (GT V94.2). (n.d.).

Pope, B. S. (2007). *Turbulence Flows*. United states of America, New York: Cambridge University Press.

Pourmohamad, M. A., Ashjari, M. A., & Khosroshahi, A. R. R. (n.d.). Recuperator Energy and Exergy Analysis in the Application of Microturbine in Cogeneration of Heat and Power Systems. *Journal of Tabriz University of Mechanical Engineering*, *46*(3), 55–66.

Sahu, M. K. (2017). Thermoeconomic investigation of power utilities : Intercooled recuperated gas turbine cycle featuring cooled turbine blades. *Energy*, *138*, 490–499. https://doi.org/10.1016/j.energy.2017.07.083

Sanaye, S., Amani, M., & Amani, P. (2018). 4E modeling and multi-criteria optimization of CCHPW gas turbine plant with inlet air cooling and steam injection. *Sustainable Energy Technologies and Assessments*, *29*(July 2017), 70–81. https://doi.org/10.1016/j.seta.2018.06.003

Sheikhbeigi, B., & Ghofrani, M. B. (2007). Thermodynamic and environmental consideration of advanced gas turbine cycles with reheat and recuperator. *International Journal of Environmental Science and Technology*, *4*(2), 253–262. https://doi.org/10.1007/BF03326282

Warnatz, J., Mass, U., & Dibble, R. W. (2006). *Combustion*. Springer.

Zaki, M., & Rajabi-Zargarabadi, M. (2014). Numerical analysis of effects of primary aeration oN NOX production in a model gas turbine combustion chamber. *Modares Mechanical Engineering*, *14*, 101–108.